Electronic Supplementary Information

Pyridyl-1,2,4-triazole diphenyl Boron complexes as efficient tuneable blue emitters

Peter Dijkstra,[a,b] Davide Angelone,[b] Elena Taknishnikh,[a] Heinrich J. Wörtche[a] Edwin Otten,[b] and Wesley R. Browne[b]*

Contents

Complex 1a

10 mL of toluene was added to a dried Schlenk tube containing 182 mg (0.75 mmol) Ph_3B and 167 mg (0.75 mmol) of **La** and heated at reflux overnight. Solvent was removed *in vacuo* and solids were dissolved in 5 mL of DCM and filtered. The filtrate was stored in a freezer and the resulting solid was filtered and washed with cold EtOH to yield a white crystalline powder, 117 mg, yield 40%. m.p. 257.3 – 257.7 °C. Elemental analysis: Calc. C 77.7, H 4.96, N 14.51 Found C 77.6, H 4.87, N 14.20. ^{1}H NMR (400 MHz, $CDCl_3$) δ 8.65 (d, *J* = 5.8, 1H), 8.31 (d, *J* = 7.7, 1H), 8.26 (m, 3H), 7.61 (t, 1H), 7.49 – 7.23 (m, 13H). ^{13}C NMR (50 MHz, $CDCl_3$) δ 169.1, 154.9, 144.6, 143.9, 142.7, 134.9, 132.9, 131.9, 129.2, 128.7, 128.1, 127.7, 126.9, 124.1, 119.4. ^{11}B NMR (128 MHz, $CDCl_3$) δ 5.21. Mass spectrum (DART): M+H 386.16 Da (23.7%) and 387.15 Da (100%) and 388.15 Da (27.6%) Calculated: m/z: 386.18 Da (24.8%) and 387.18 Da (100%) and 388.18 Da (28.7%) Resp. ^{10}B, ^{11}B and ^{11}B with ^{13}C

.

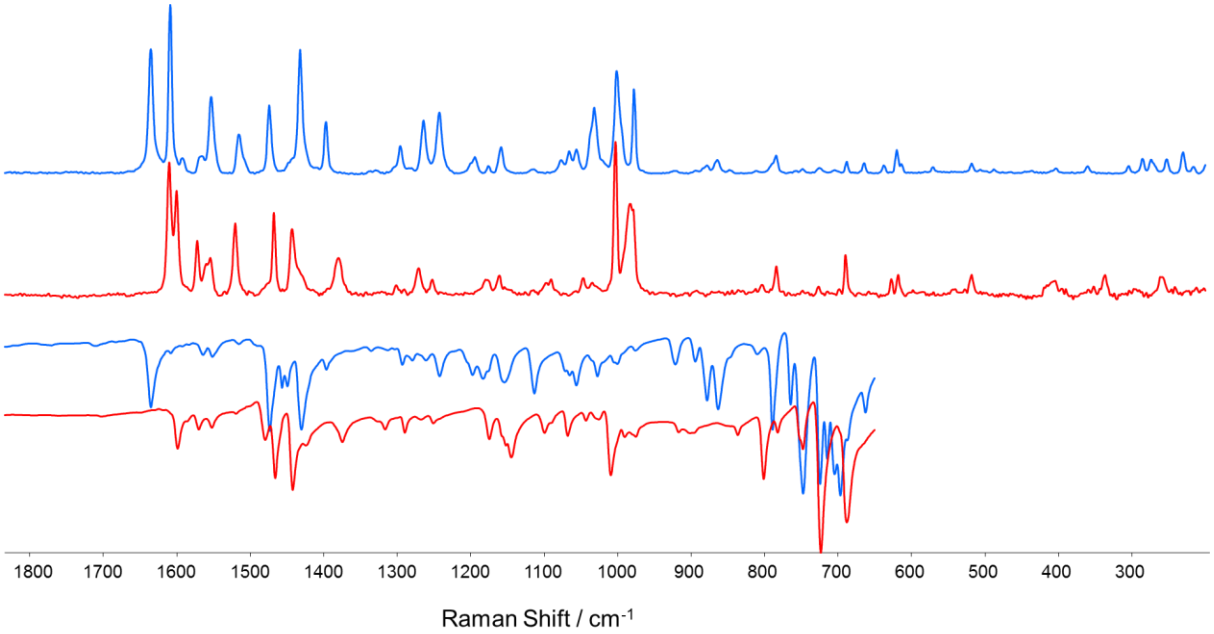

Fig. S1 Raman spectra (λ_{exc} 785 nm) and FTIR spectra of ligand **La** (red) and complex **1a** (blue)

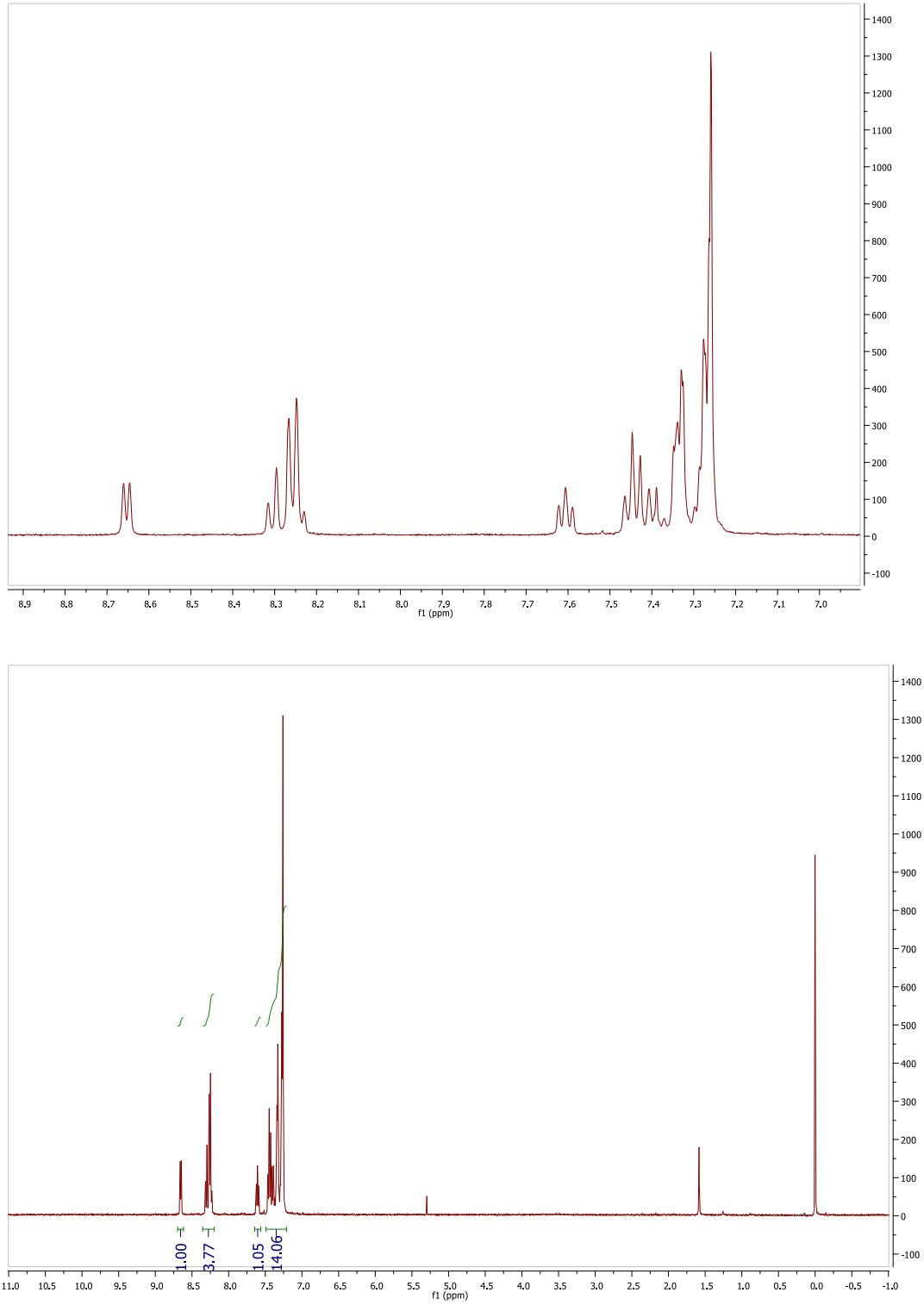

Fig. S2 ^{1}H NMR spectrum (400 MHz) of complex **1a** in $CDCl_3$.

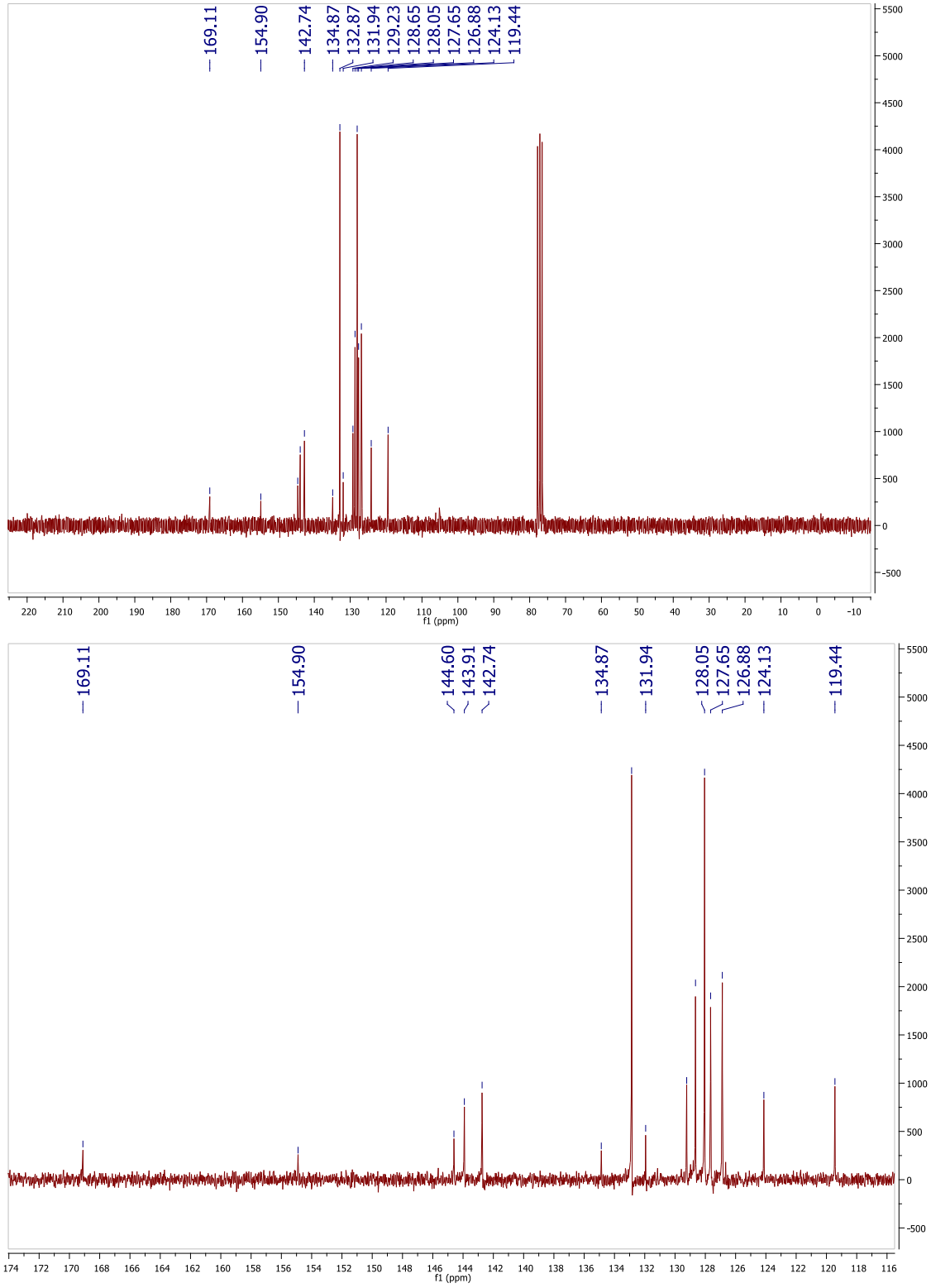

Fig. S3 ^{13}C NMR (50 MHz) spectrum of complex **1a** in $CDCl_3$.

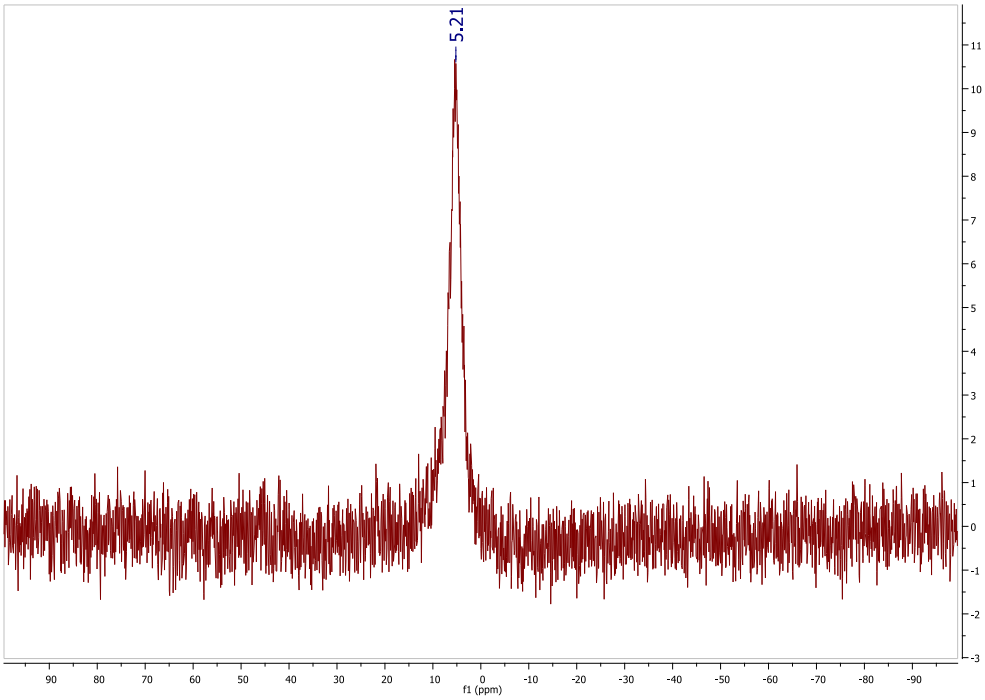

Fig. S4 ^{11}B NMR (128 MHz, $CDCl_3$) δ 5.21

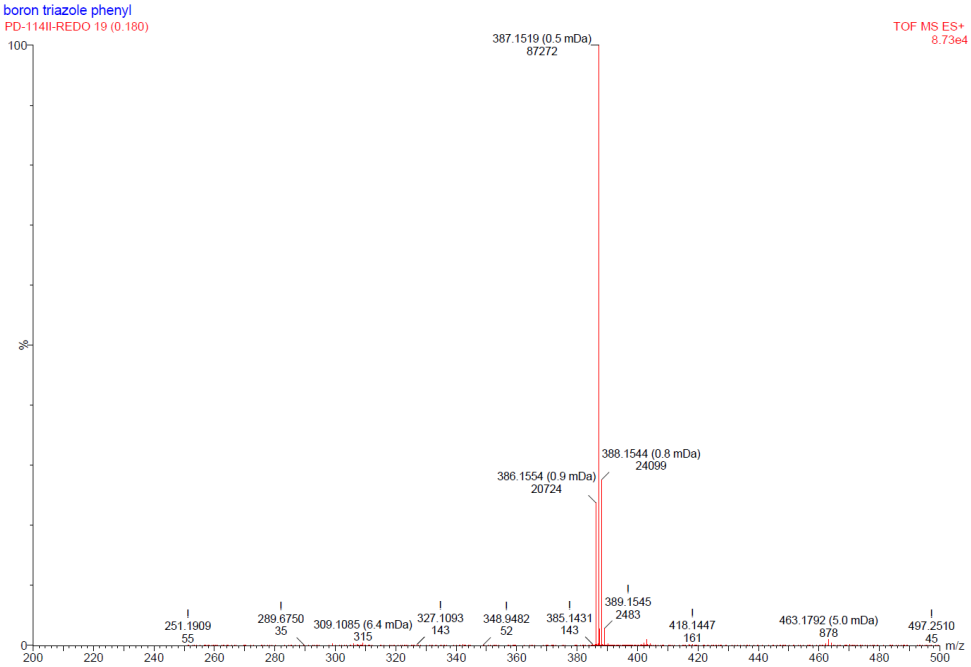

Fig. S5 Mass spectrum (DART) of complex **1a**

Complex 1b

15 mL of toluene was added to a dried Schlenk tube containing 500 mg (2.0 mmol) Ph_3B and 443 mg (1.9 mmol) of **Lb** and heated at reflux overnight. Solvent was removed *in vacuo* and solids were dissolved in 5 mL of EtOAc and filtered. The filtrate was stored in a freezer and the resulting solid was filtered and washed with cold EtOH to yield a white crystalline powder, 236 mg, yield 35%. m.p. 2578.4 – 259 °C. Elemental analysis: Calc. C 78.0, H 5.29 , N 14.0 Found C 76.6, H 4.87, N 14.2. ^{1}H NMR (400 MHz, $CDCl_3$) δ 8.63 (d, *J* = 5.8 Hz, 1H), 8.28 (d, *J* = 8.0 Hz, 1H), 8.22 (td, *J* = 8.0, 1.2 Hz, 1H), 8.14 (d, *J* = 8.1 Hz, 2H), 7.57 (ddd, *J* = 7.2, 5.8, 1.2 Hz, 1H), 7.38 – 7.21 (m, 12H), 2.40 (s, 3H). ^{13}C NMR (101 MHz, $CDCl_3$) δ 169.2, 154.8, 144.6, 143.9, 142.7, 139.2, 132.9, 129.4, 129.2, 128.0, 127.6, 126.8, 124.1, 119.4, 21.6. DART MS spectrum: M+H 400.23 Da (27.7%) and 401.23 Da (100%) and 402.23 Da (29.00%) Calculated: m/z: 400.20 (24.8%), 401.19 (100.0%), 402.20 (29.3%) Resp ^{10}B, ^{11}B and ^{11}B with ^{13}C.

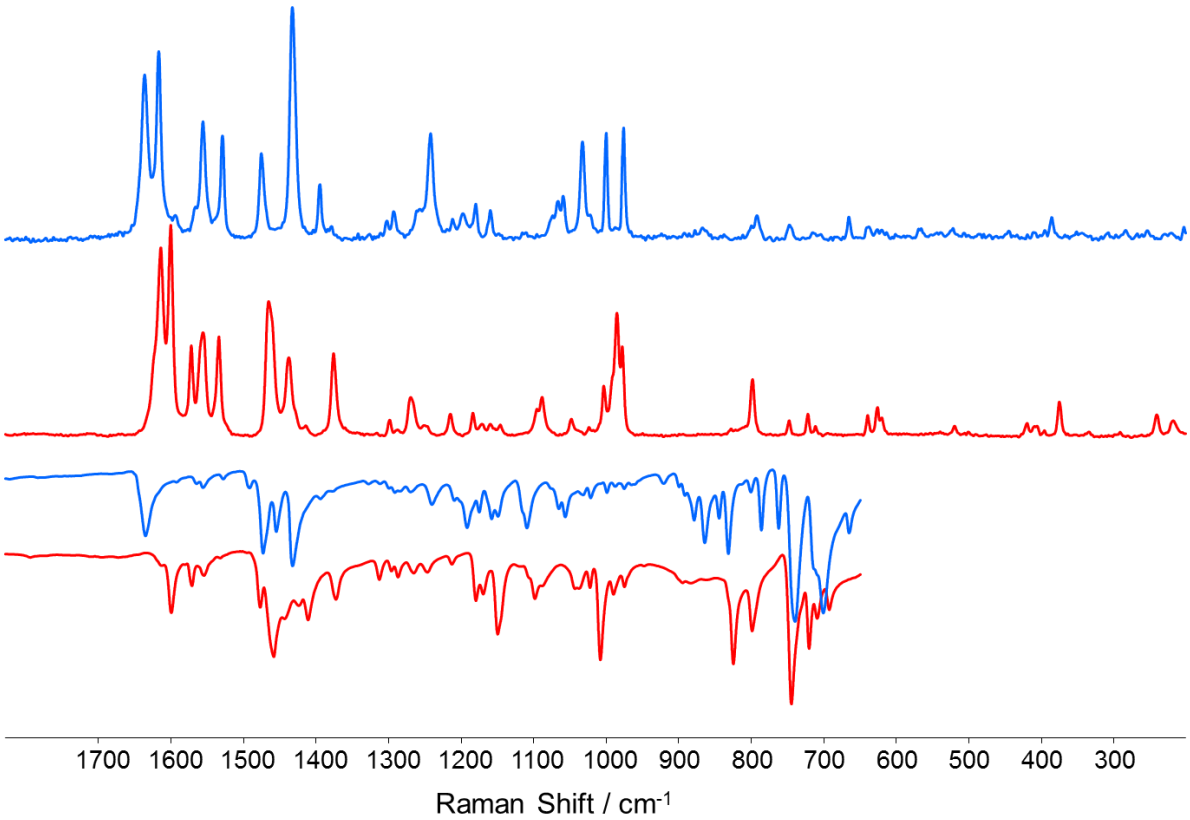

Fig. S6 Raman spectra (λ_{exc} 785 nm) and FTIR spectra of ligand **Lb** (red) and complex **1b** (blue)

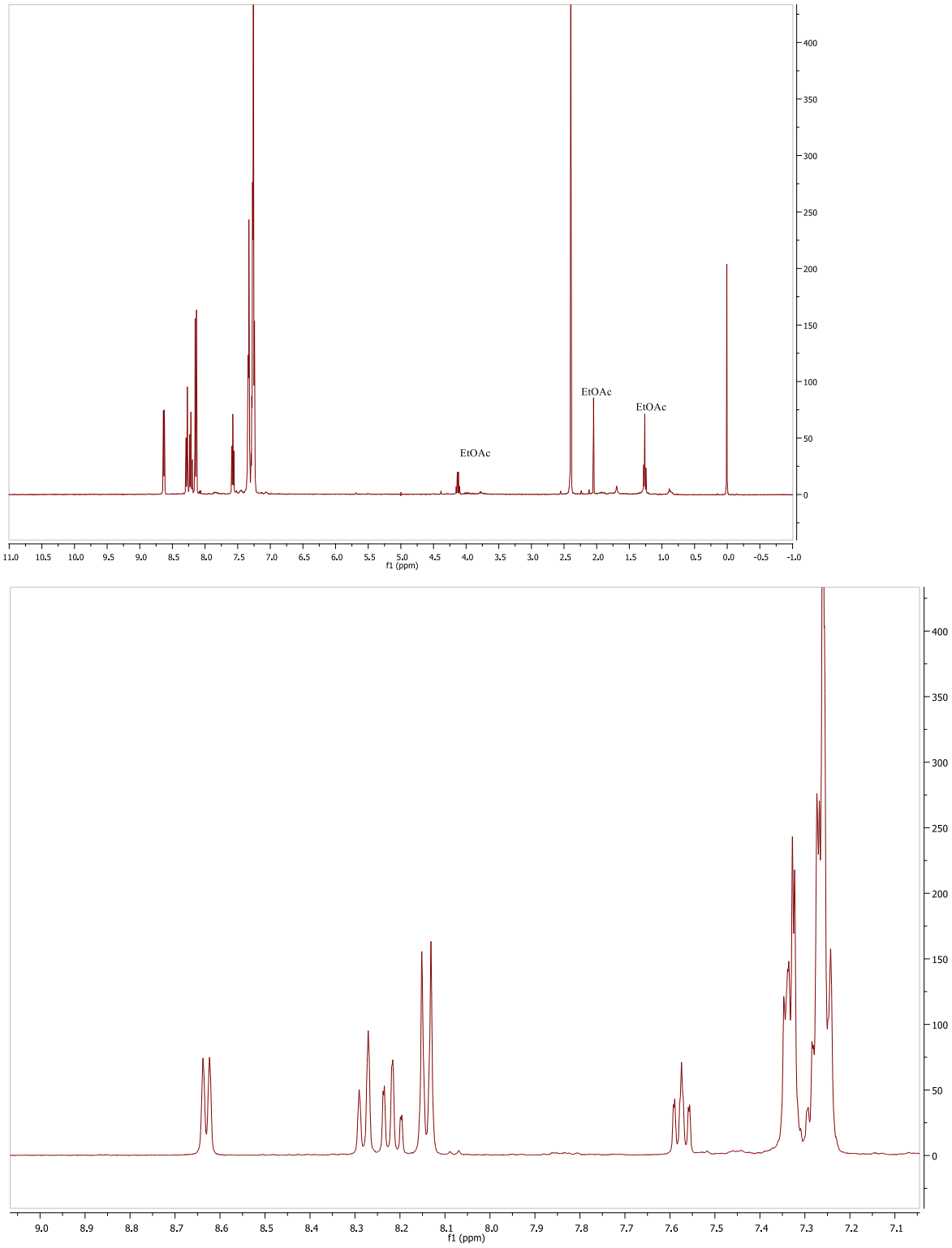

Fig. S7 ^{1}H NMR (400 MHz, $CDCl_3$) spectrum of **1b**

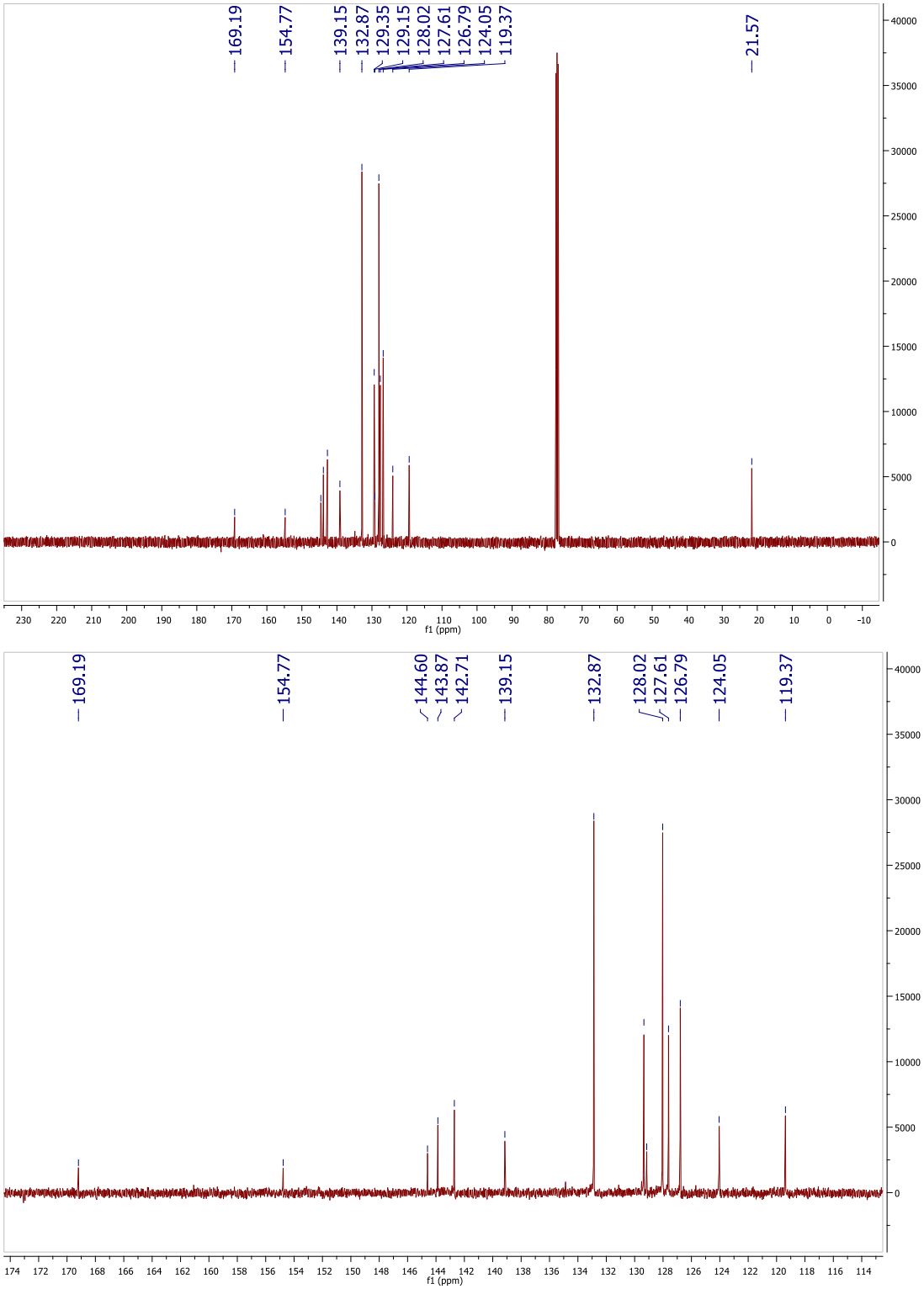

Fig. S8 ^{13}C NMR (101 MHz, $CDCl_3$) spectrum of **1b**

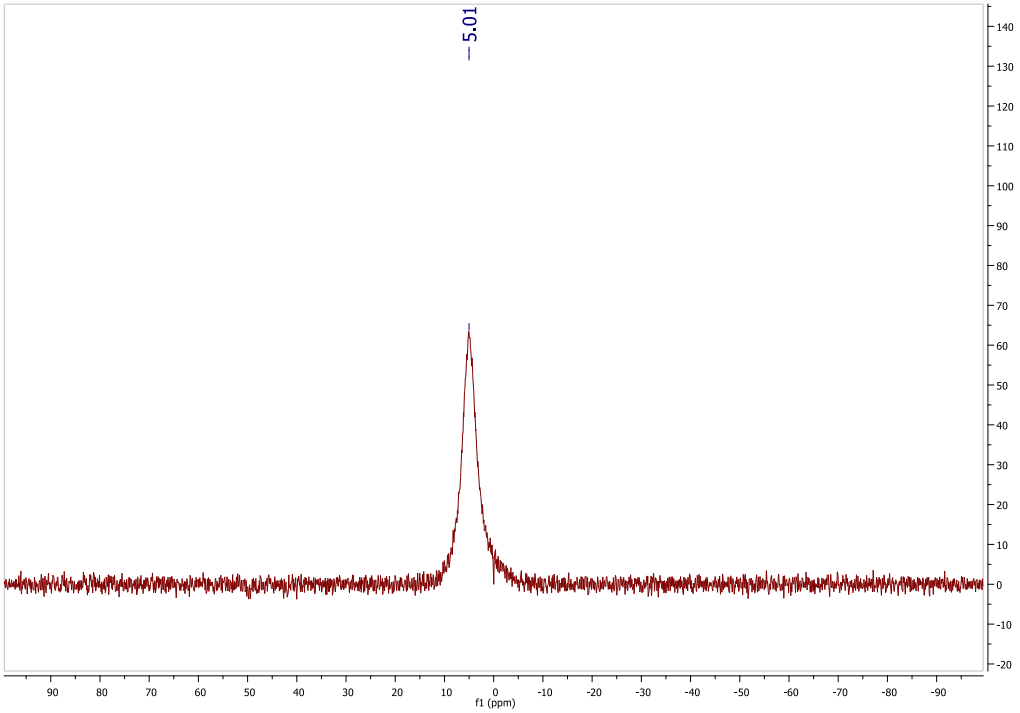

Fig. S9 ^{11}B NMR (128 MHz, $CDCl_3$) δ 5.01

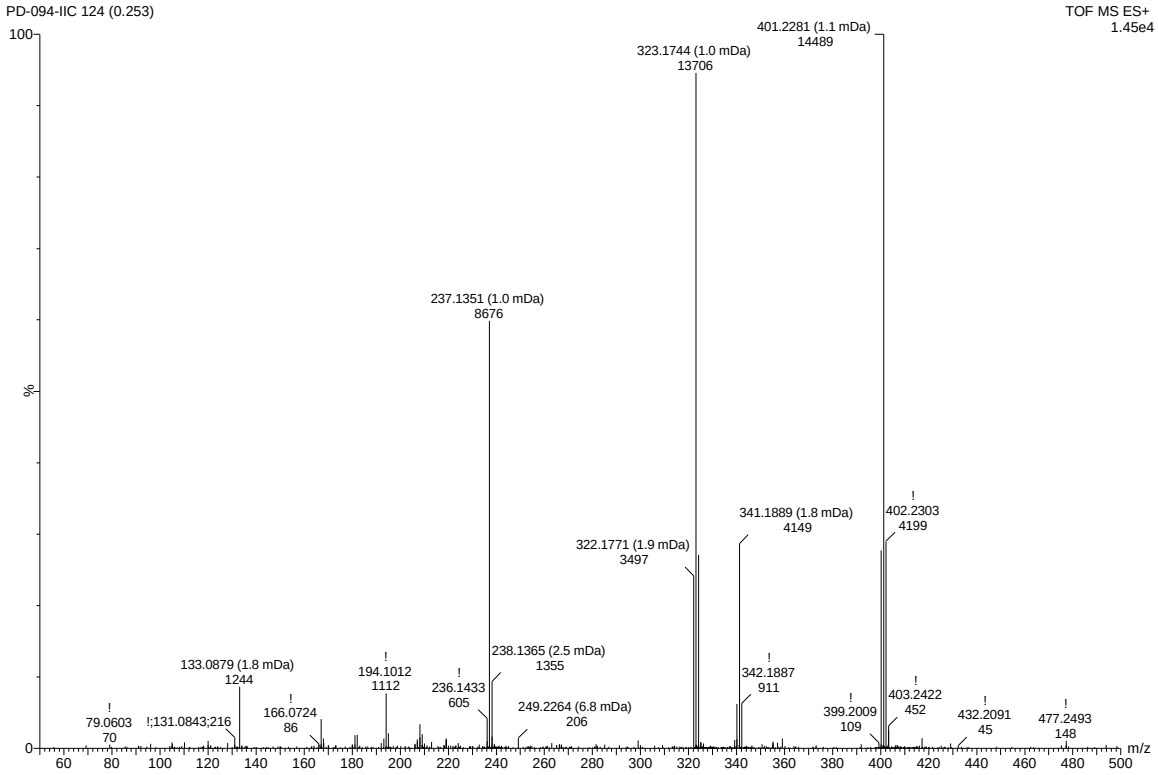

Fig. S10 DART MS spectrum of complex **1b**

Complex 1c

10 mL of toluene was added to a dried Schlenk tube containing 148 mg (0.6 mmol) Ph_3B and 350 mg (1.4 mmol) of **Lc** and heated at reflux overnight. Solvent was removed *in vacuo* and solids were dissolved in 5 mL of THF and filtered. The filtrate was stored in a freezer and the resulting solid was filtered and washed with cold EtOH to yield a white crystalline powder, 160 mg, yield 27%. m.p. 236.3 – 237.4 °C. Elemental analysis: Calc. C 75.02, H 5.08, N 13.48 Found C 72.35, H 5.53, N 11.85. ^{1}H NMR (400 MHz, $CDCl_3$) δ 8.61 (d, *J* = 5.6, 1H), 8.26 (d, *J* = 7.8, 1H), 8.19 (t, *J* = 7.9, 3H), 7.55 (t, *J* = 6.5, 1H), 7.40 – 7.16 (m, 10H), 6.97 (d, *J* = 8.6, 2H), 3.85 (s, 3H). ^{13}C NMR (101 MHz, $CDCl_3$) δ 169.0, 160.6, 154.7, 144.7, 143.9, 142.7, 134.9, 132.9, 131.2, 128.3, 128.0, 127.6, 124.8, 124.0, 119.3, 114.0, 55.5. ^{11}B NMR (128 MHz, $CDCl_3$) δ 5.21. Mass Spec. (DART): M+H 416.14 Da (14%) 417.16 Da (100%) and 418.17 Da (17%) Calculated: m/z: 416.19 (24.8%), 417.19 (100.0%), 418.19 (29.9%), Resp ^{10}B, ^{11}B and ^{11}B with ^{13}C.

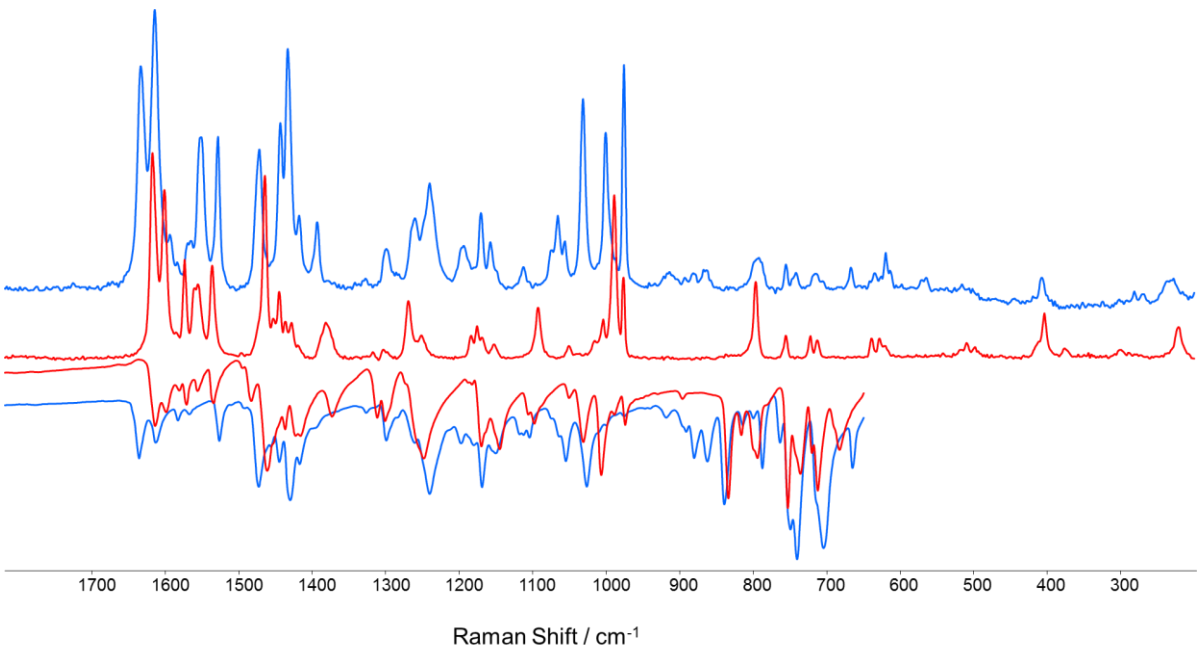

Fig. S11 Raman spectra (λ_{exc} 785 nm) and FTIR spectra of ligand **Lc** (red) and complex **1c** (blue)

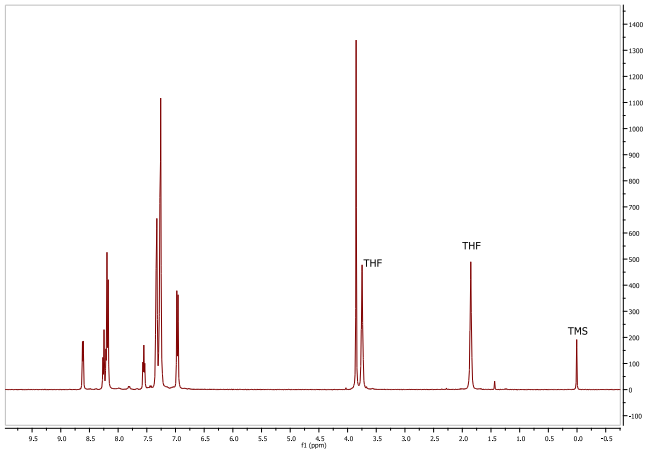

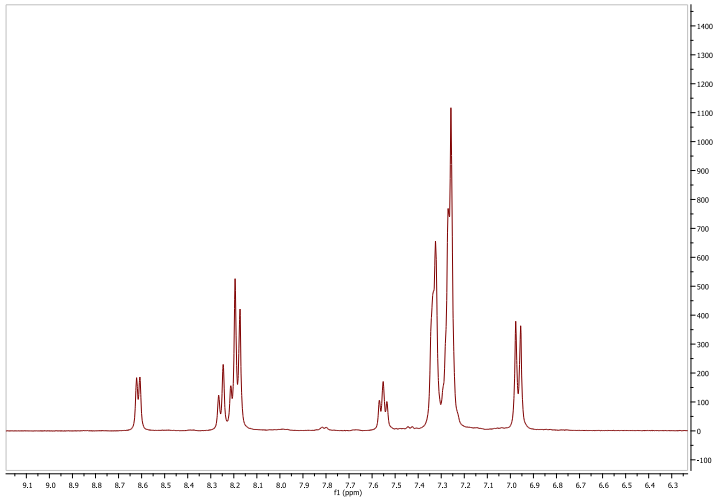

Fig. S12 ^{1}H NMR (400 MHz, $CDCl_3$) spectrum of **1c**

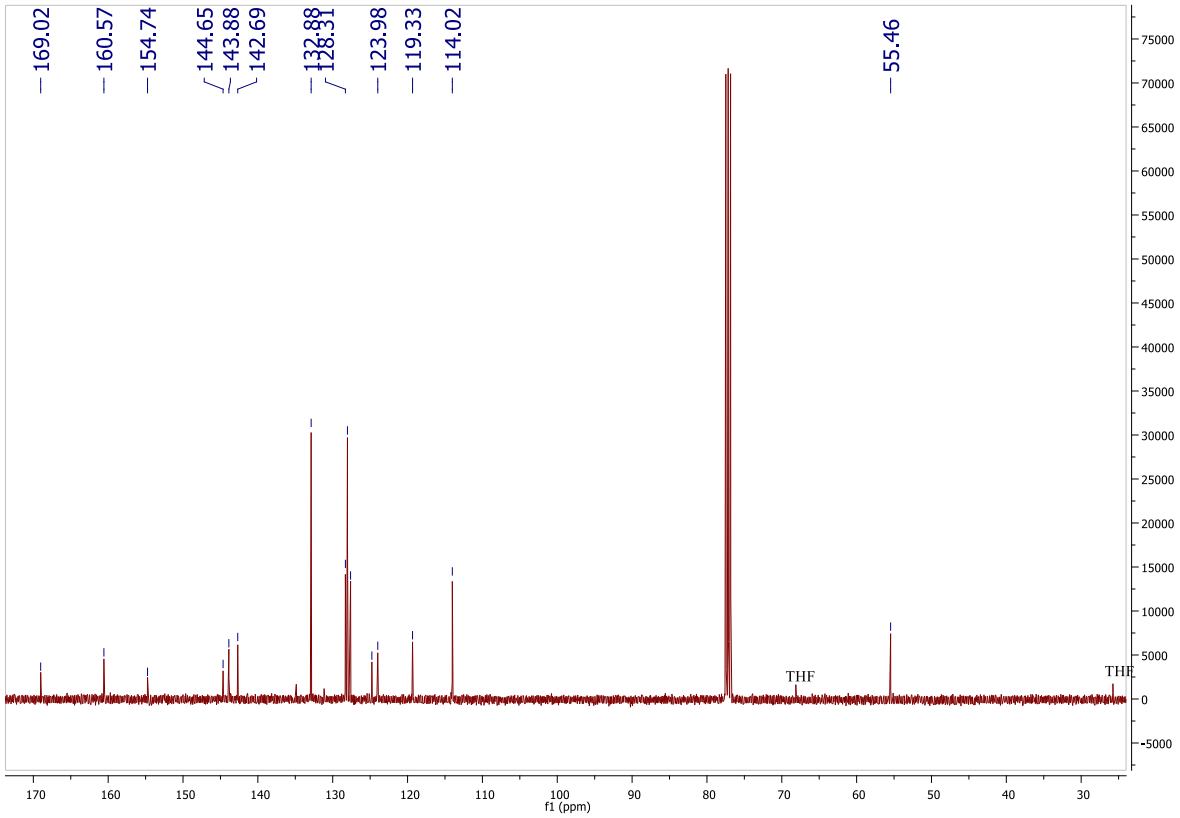

Fig. S13 ^{13}C NMR (101 MHz, $CDCl_3$) spectrum of **1c**

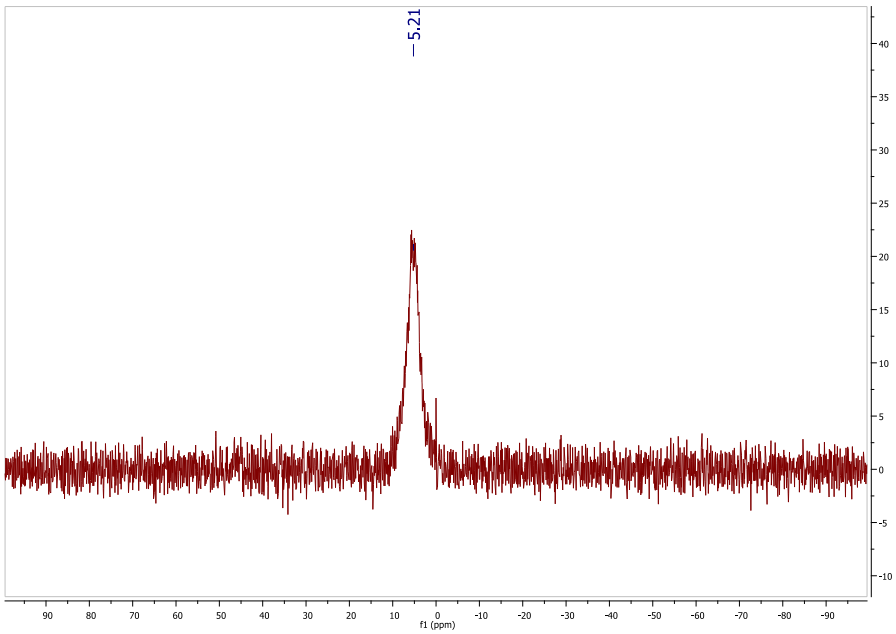

Fig. S 14 ^{11}B NMR (128 MHz, $CDCl_3$) spectrum of **1c**

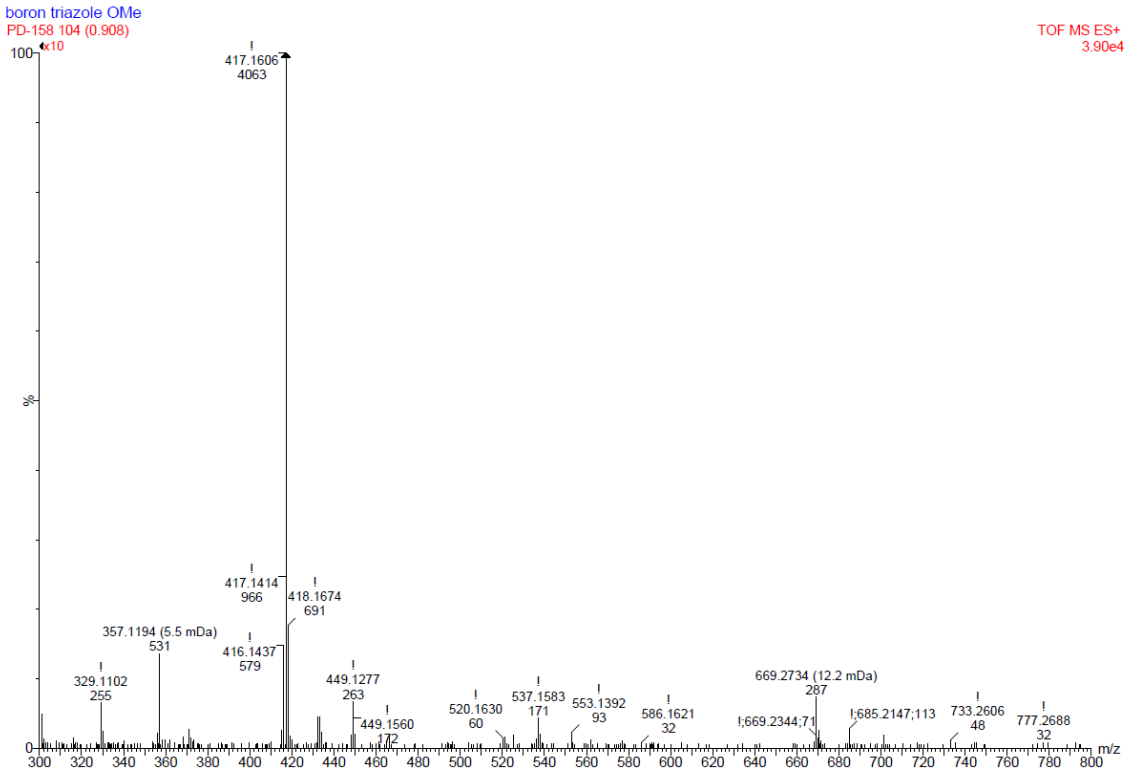

Fig. S15. Mass Spectrum (DART) of **1c.** Note that higher m/z signals are also present without 1c

Complex 1d

15 mL of toluene was added to a dried Schlenk tube containing 205 mg (0.85 mmol) Ph_3B and 200 mg (0.85 mmol) **Lb** and the mixture heated at reflux overnight. Solvent was removed *in vacuo* and solids were dissolved in 5 mL of DCM and filtered. The filtrate was in a freezer. The solid obtained was recovered by filtration and washed with cold EtOH to yield a white crystalline powder, 123 mg, yield 35%, m.p. 278.0-278.5 oC. Elemental analysis Calc :C 78.0, H 5.29, N 14.00. Found C 76.6, H 5.14, N 13.63. ^{1}H NMR (400 MHz, cdcl$_3$) δ 8.34 – 8.03 (m, 4H), 7.46 – 7.12 (m, 15H), 2.48 (s, 3H). ^{13}C NMR (50 MHz, CDCl$_3$) δ 168.8, 157.5, 145.2, 142.6, 134.9, 133.8, 132.0, 131.0, 129.0, 128.5, 128.0, 127.9, 127.5, 126.8, 126.6, 126.2, 116.9, 22.4. ^{11}B NMR (128 MHz, CDCl$_3$) δ 5.43 (s, 1B). DART-MS: M+H 400.17 Da (32.0%) and 401.16 Da (100%) and 402.17 Da (26.4%) Calculated: m/z: 400.20 (24.8%), 401.19 (100.0%), 402.20 (29.3%), Resp ^{10}B, ^{11}B and ^{11}B with ^{13}C

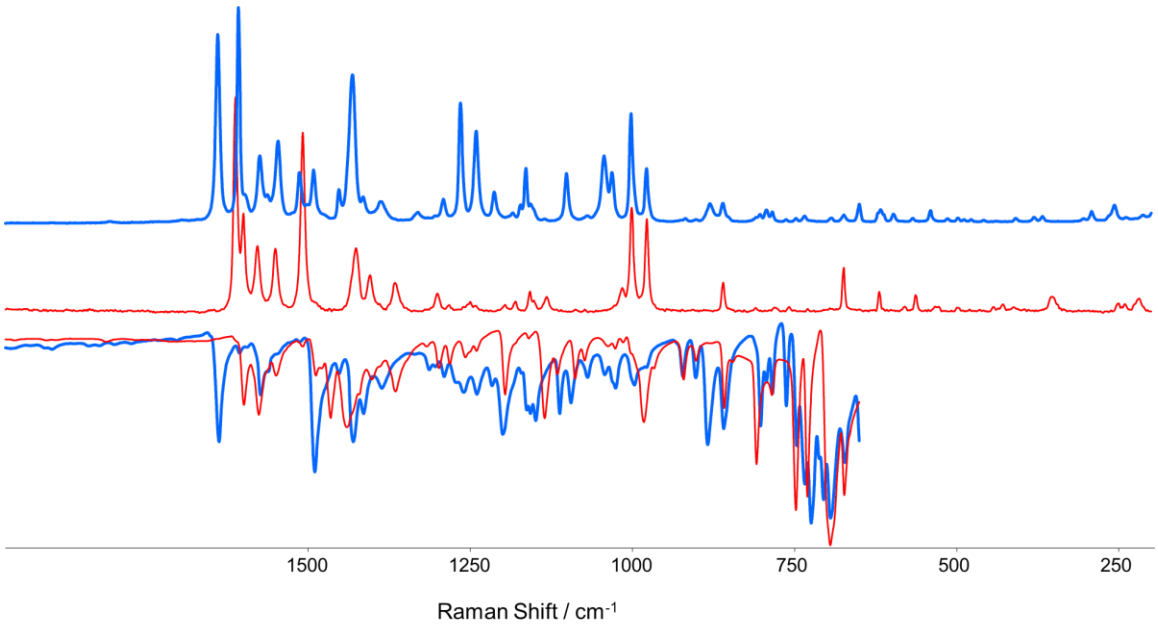

Fig. S16 Raman spectra (λ_{exc} 785 nm) and FTIR spectra of ligand **Ld** (red) and complex **1d** (blue)

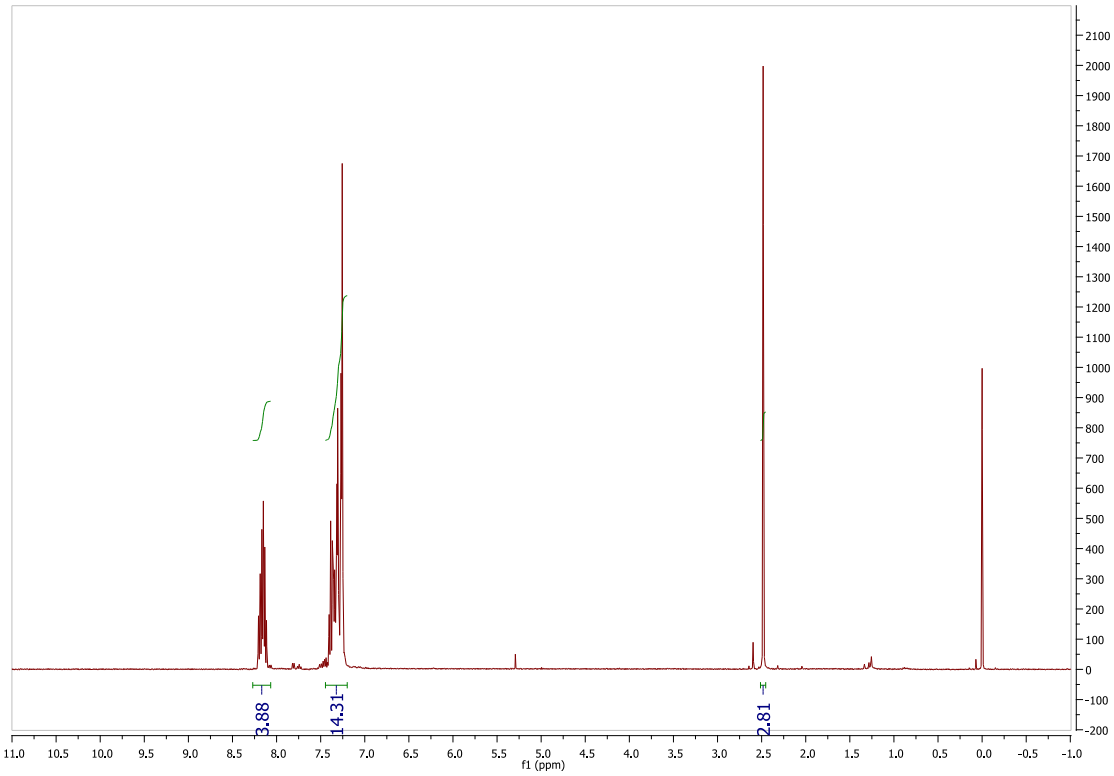

Fig S17 ^{1}H NMR (400 MHz, $CDCl_3$) spectrum of **1d**.

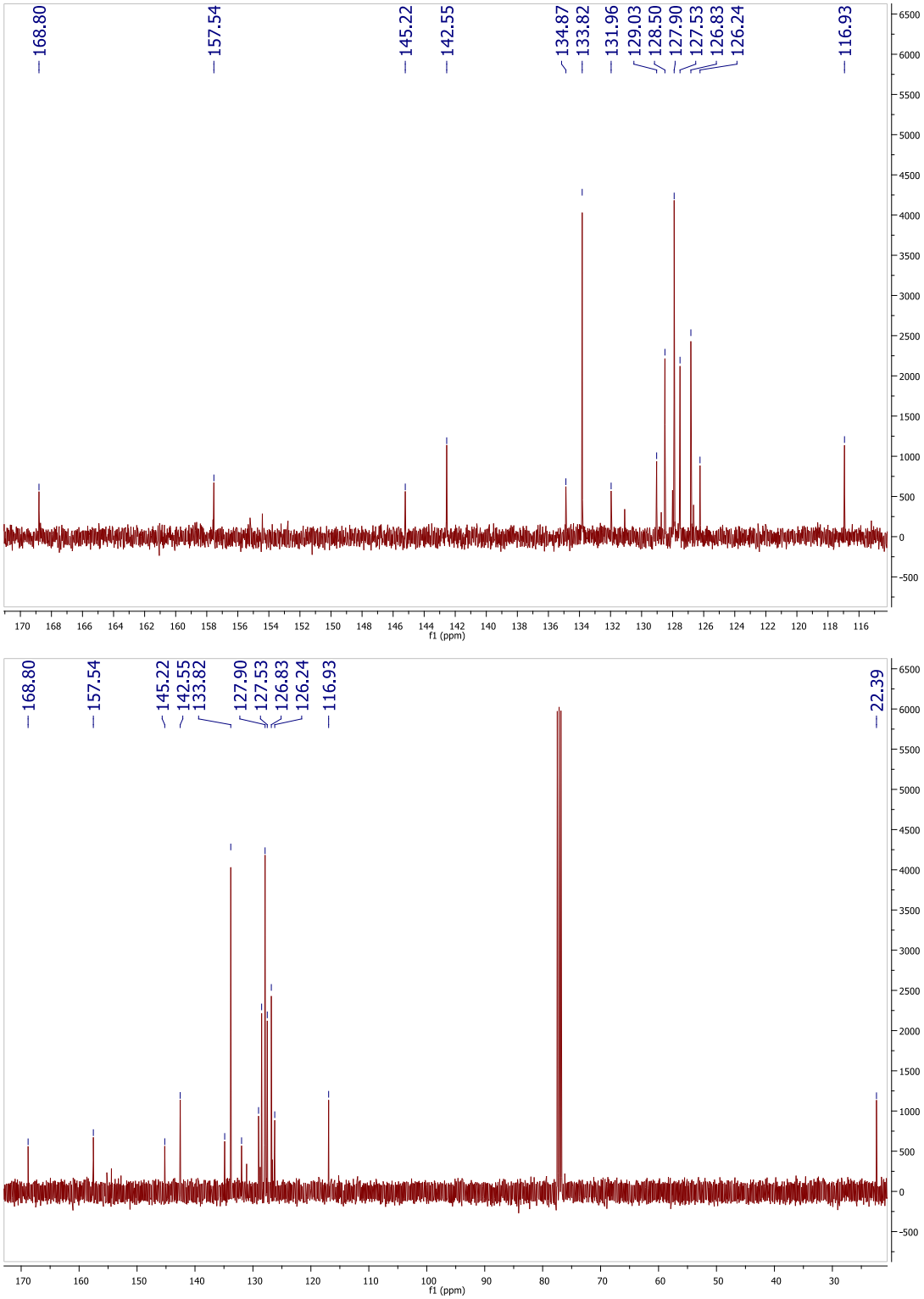

Fig S18 ^{13}C NMR (50 MHz, $CDCl_3$) spectrum of **1d**.

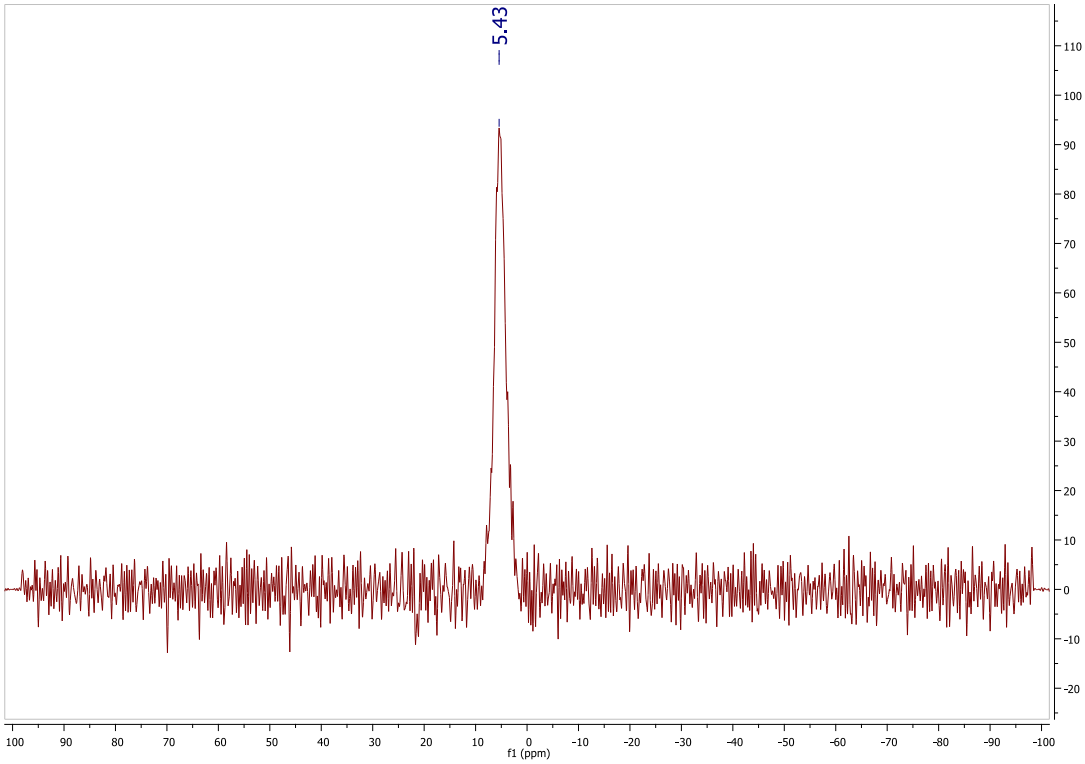

Fig. S19 ^{11}B NMR (128 MHz, $CDCl_3$) spectrum of **1d**

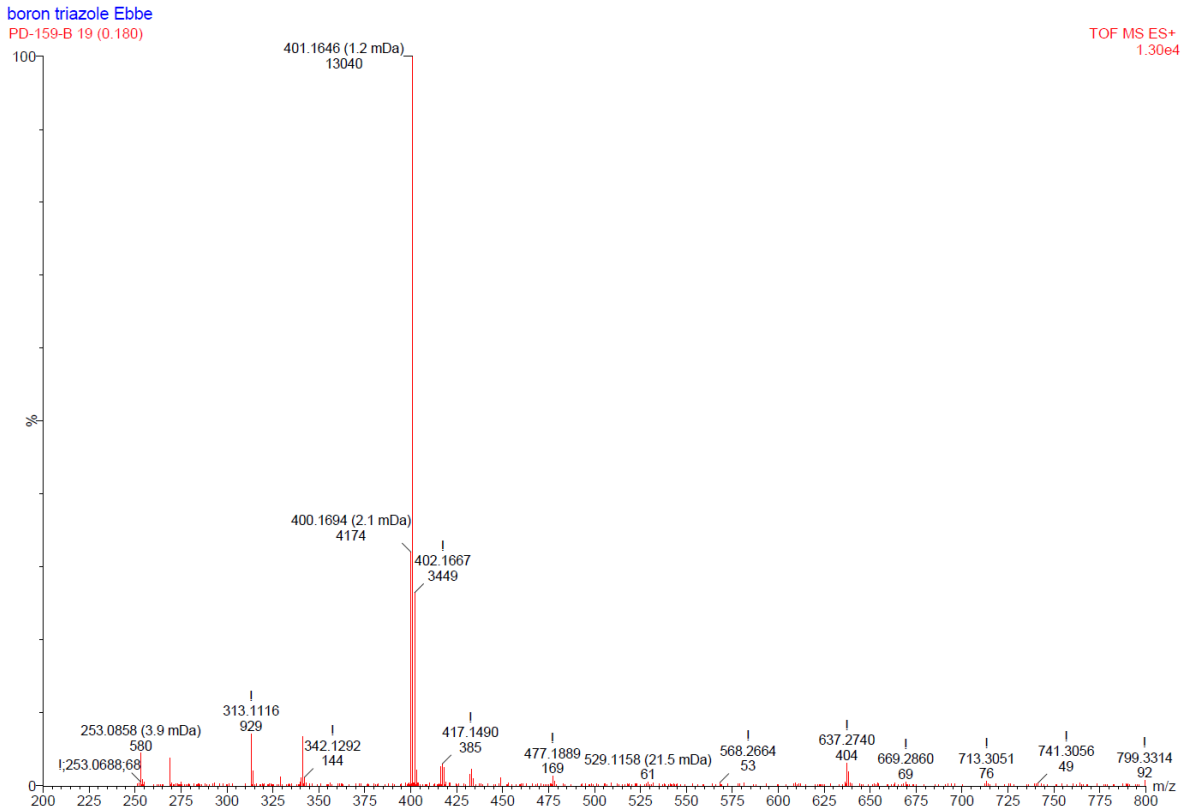

Fig 20 DART-MS spectrum of complex **1d**

Complex 1e

20 mL of dry THF was added to a dried Schlenk tube containing 0.69 g (4.3 mmol) of **Le**. 1.06 g (4.4 mmol) Ph_3B was added, which resulted in the immediate appearance of a milky white solution. After stirring for 1 h at room temperature the solvent was removed *in vacuo*. All solids were dissolved in DCM and loaded on celite. The sample was purified by column chromatography on silica with pentane/EtOAc (0-100%) as eluent. The blue fluorescent fraction was collected and recrystallized from EtOAc, yielding 360 mg of a white solid, yield 26%. M. P. 239.5-240.5 ^{o}C. Elemental analysis, calc: C 74.1, H 5.29, N 17.28 Measured: C 73.9, H 5.30, N 17.17. ^{1}H NMR (400 MHz, $CDCl_3$) δ 8.63 (d, *J* = 5.7, 1H), 8.22 (m, 2H), 7.59 (ddd, *J* = 7.3, 5.8, 1.5, 1H), 7.27 (m, 10H), 2.59 (s, 3H). ^{13}C NMR (101 MHz, $CDCl_3$) δ 167.6, 154.3, 144.6, 143.9, 142.7, 132.7, 128.0, 127.6, 124.0, 119.2, 14.8. ^{11}B NMR (128 MHz, $CDCl_3$) δ 4.93. Mass spec. (DART): M+H 324.14 Da (23.8%) and 325.14 Da (100%) and 326.14 Da (25.2%) Calculated: m/z: 324.17 (24.8%), 324.16 (100.0%), 326.17 (22.4%) Resp M+H for ^{10}B, ^{11}B and ^{11}B with ^{13}C

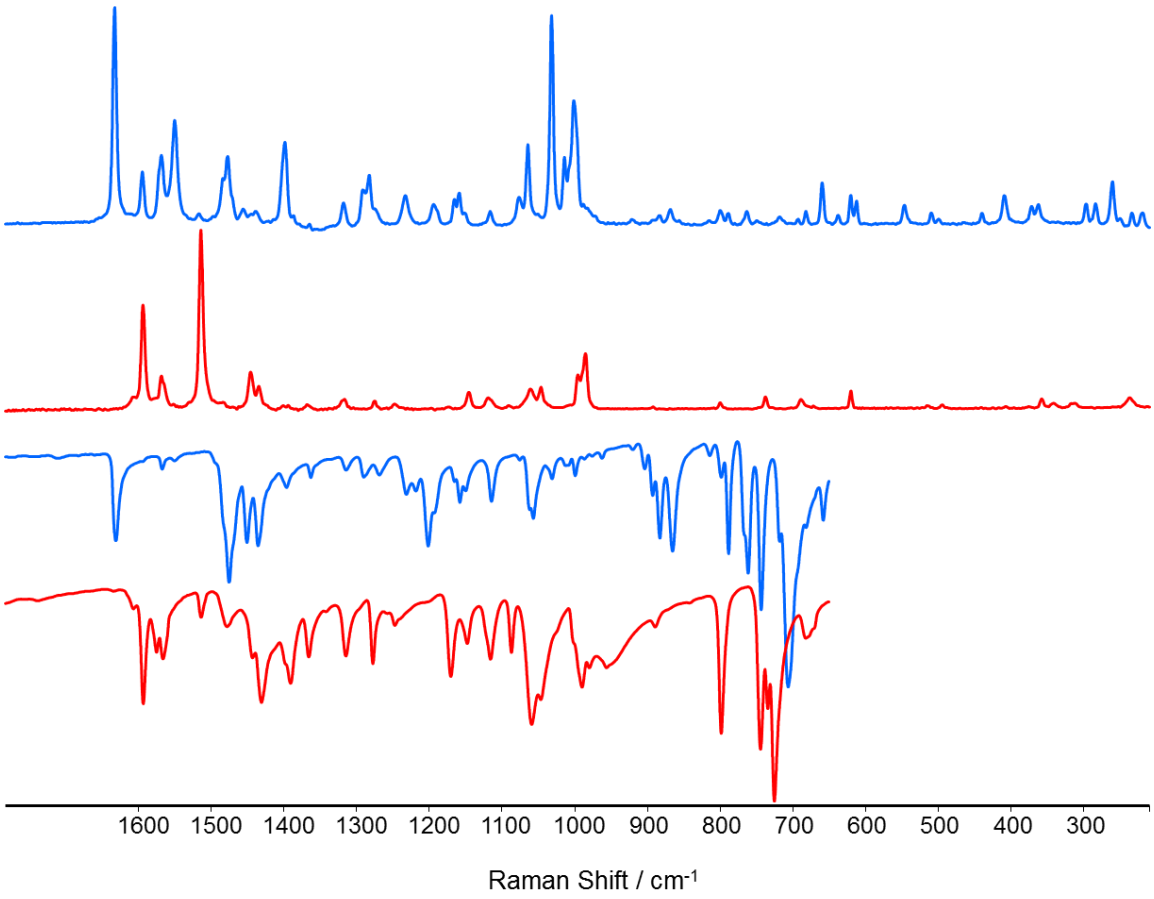

Fig. S21 Raman spectra (λ_{exc} 785 nm) and FTIR spectra of ligand **Le** (red) and complex **1e** (blue)

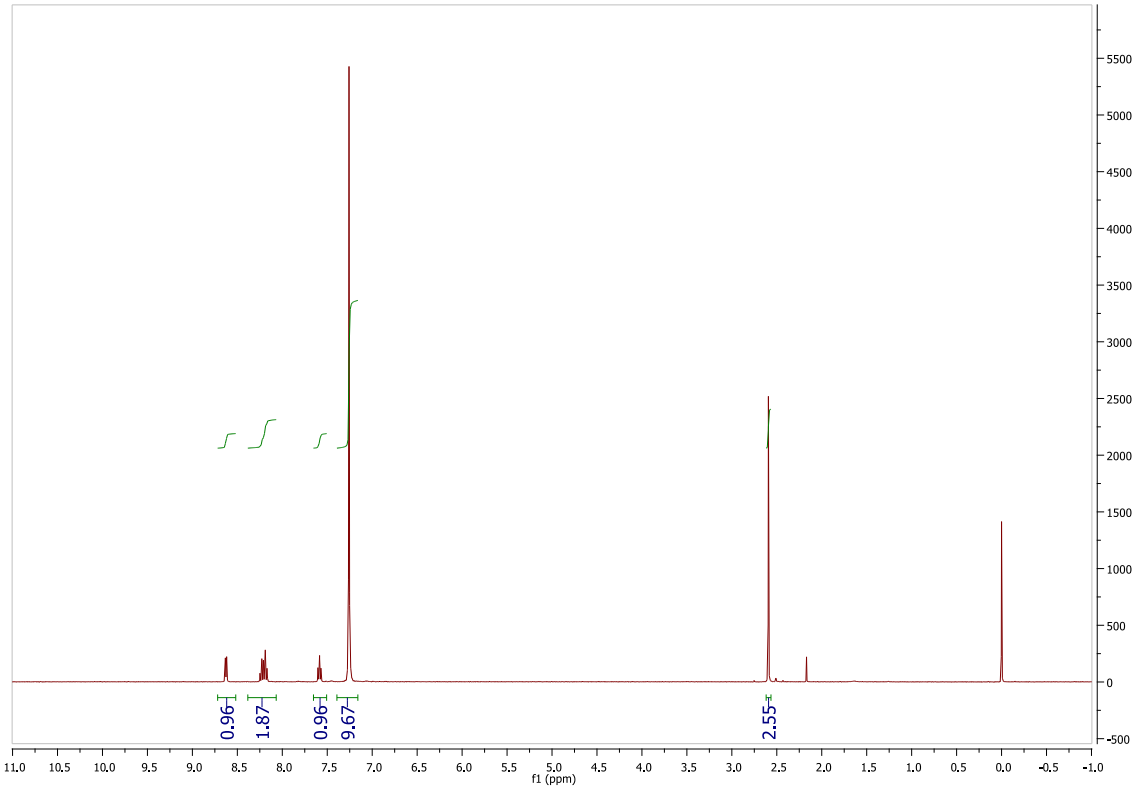

Fig. S22 ^{1}H NMR (400 MHz, $CDCl_3$) spectrum of **1e**.

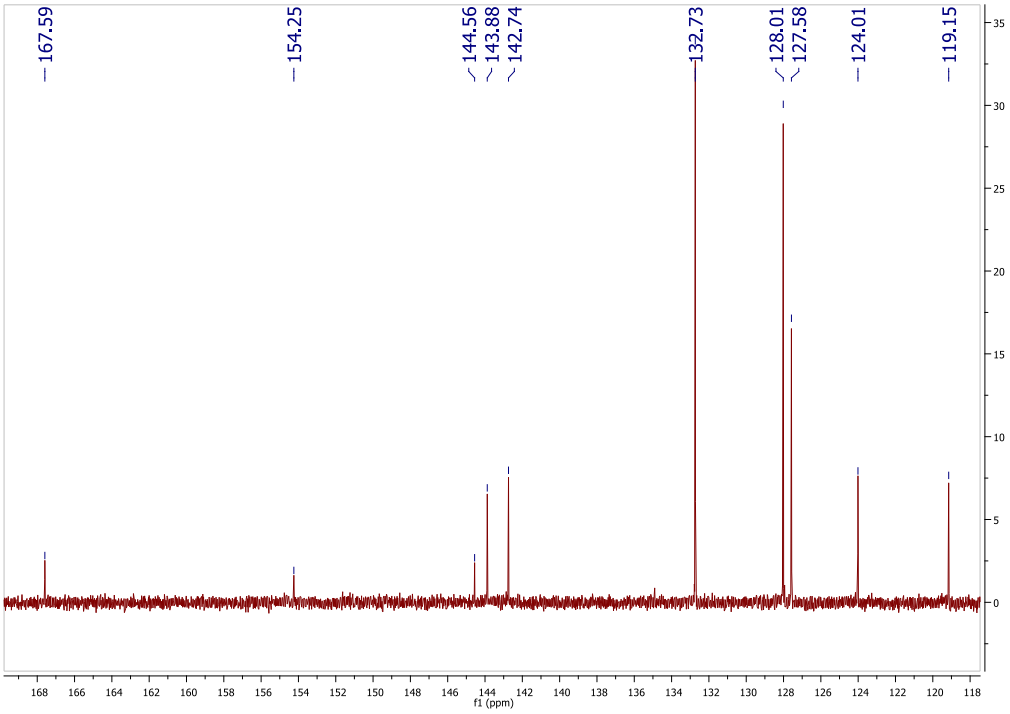

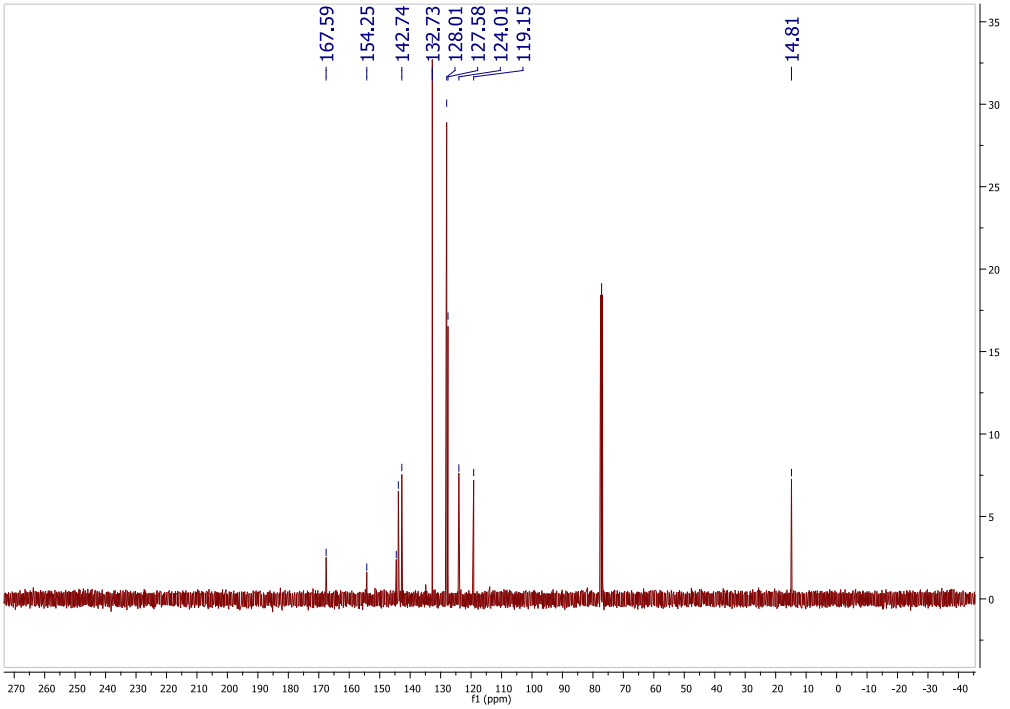

Fig. S23 ^{13}C NMR (101 MHz, $CDCl_3$) spectrum of **1e**.

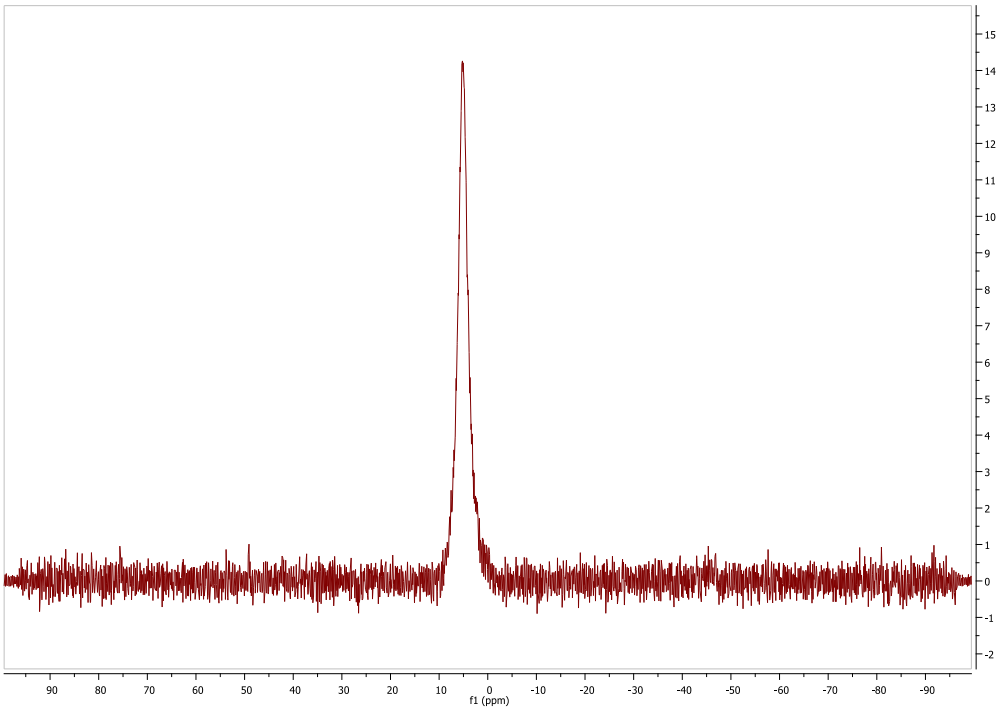

Fig. S24 ^{11}B NMR (128 MHz, $CDCl_3$) spectrum of **1e**

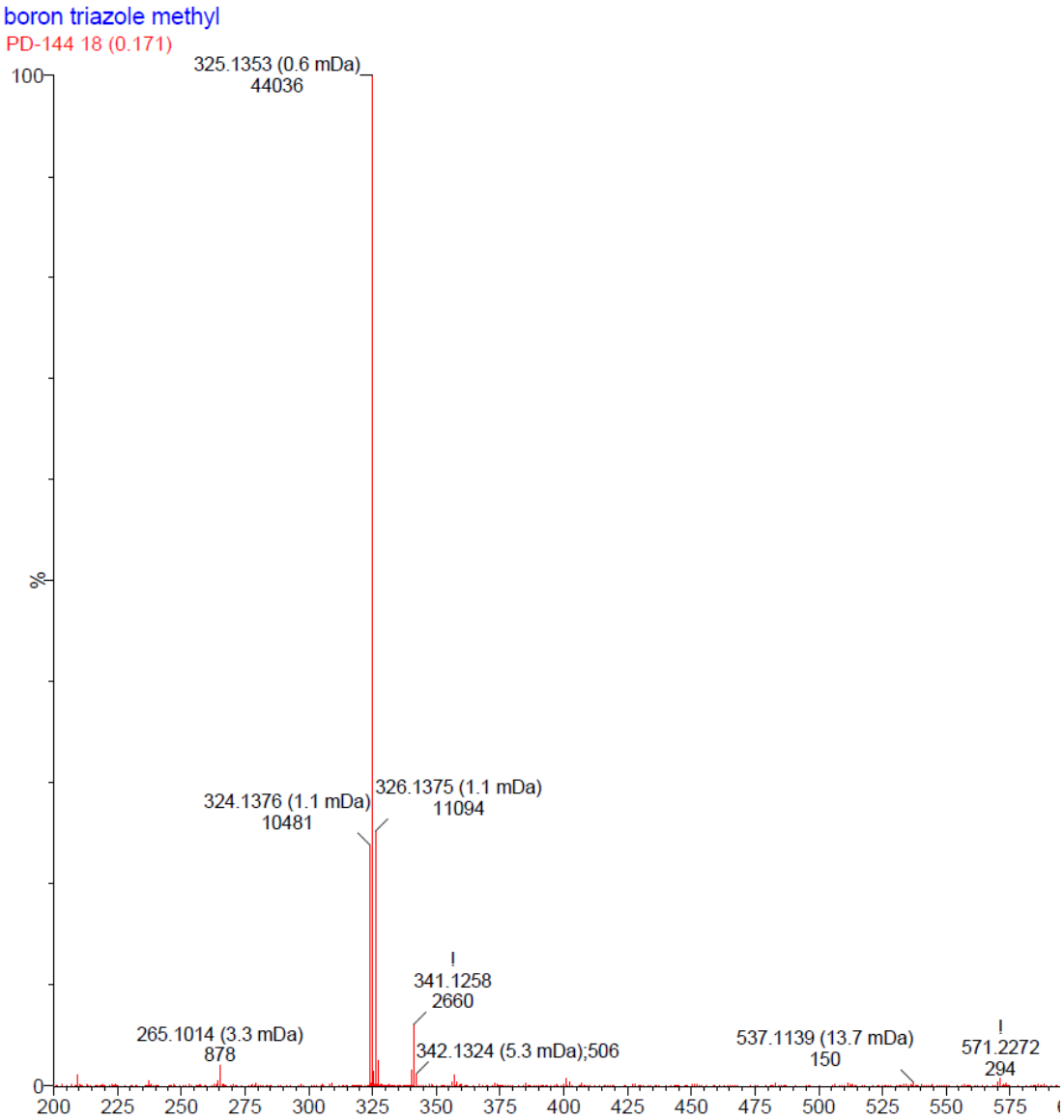

Fig. S25 Mass spectrum (DART) of **1e**

X-ray crystallography.

A suitable crystals of **1a** was mounted on a cryo-loop transferred into the cold nitrogen stream of a Bruker D8 Venture diffractometer. The final unit cell was obtained from the xyz centroids of 9705 reflections after integration. Intensity data were corrected for Lorentz and polarisation effects, scale variation, for decay and absorption: a multiscan absorption correction was applied, based on the intensities of symmetry-related reflections measured at different angular settings (*SADABS)*.[1] The structures were solved by direct methods using the program *SHELXS*.[2] The hydrogen atoms were generated by geometrical considerations and constrained to idealised geometries and allowed to ride on their carrier atoms with an isotropic displacement parameter related to the equivalent displacement parameter of their carrier atoms. Structure refinement was performed with the program package *SHELXL.*[2] Crystal data and details on data collection and refinement are presented in Table S1.

Table S1. Crystallographic data for **1e**.

	1e
chem formula	$C_{20}H_{17}BN_4$
M_r	324.19
cryst syst	orthorhombic
color, habit	colourless, block
size (mm)	0.37 x 0.23 x 0.23
space group	$P2_12_12_1$
a (Å)	9.1229(9)
b (Å)	10.9815(11)
c (Å)	16.3366(17)
V (Å^3)	1636.7(3)
Z	4
ρ_{calc}, g.cm^{-3}	1.316
μ(Mo K_α), mm^{-1}	0.080
F(000)	680
temp (K)	100(2)
θ range (°)	2.90-27.15
data collected (h,k,l)	-11:11, -14:14, -20:20
min, max transm	0.9712, 0.9819
rflns collected	42384
indpndt reflns	3624
observed reflns $F_o \geq 2.0\ \sigma\ (F_o)$	3515
R(F) (%)	3.03
wR(F^2) (%)	7.79
GooF	1.042
weighting a,b	0.0431, 0.4723
params refined	227
min, max resid dens	-0.117, 0.257

Cyclic voltammetry

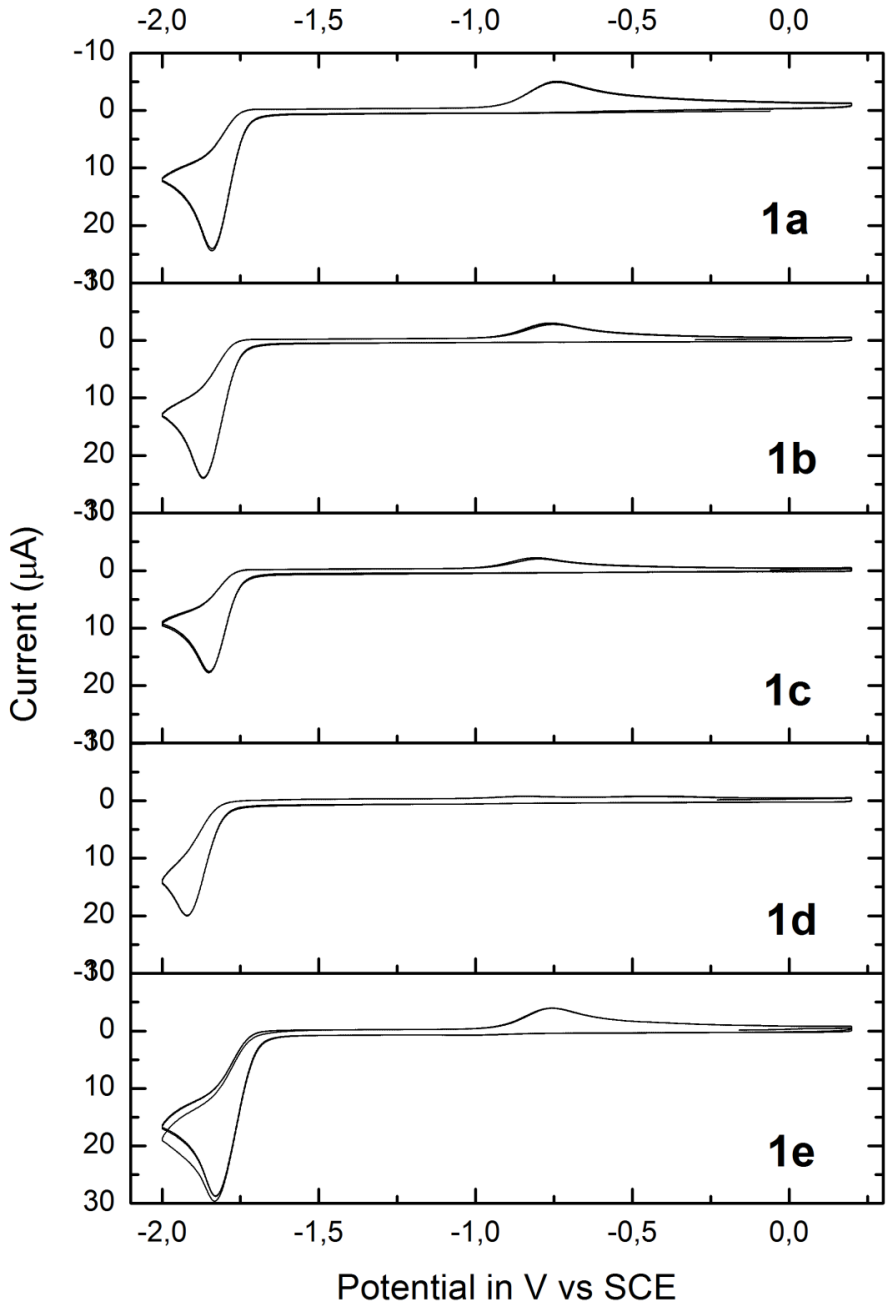

Fig. S26 Cyclic voltammetry of **1a-e** in CH_2Cl_2 with 0.1 mM $TBAPF_6$ at a GC electrode and platinum counter electrode. Scan rate 0.1 V s^{-1}.

Coordinates for calculated structure of 1e

Calculations were carried out using the Gaussian09c[3] software package

A geometry optimisation was carried out using DFT rb3lyp/6-311++g(2d,2p)

Singlet with zero charge

B	8.227609000	5.324804000	5.100119000
C	7.586659000	6.573906000	5.892449000
C	6.211525000	6.664338000	6.146581000
C	8.384080000	7.649288000	6.310251000
C	9.710247000	4.871751000	5.547279000
C	11.230556000	4.286114000	7.363386000
C	9.994147000	4.736826000	6.914455000
C	6.468770000	8.831877000	7.172973000
C	7.838044000	8.766134000	6.936494000
C	11.975931000	4.084418000	5.091005000
C	10.730477000	4.528281000	4.651436000
C	5.656955000	7.773071000	6.779745000
C	12.230693000	3.961715000	6.451476000
N	7.262220000	4.102110000	4.960996000
N	6.081434000	2.764626000	3.645358000
N	8.185526000	5.667991000	3.484762000
N	6.732490000	3.183525000	5.780702000
C	7.411561000	4.794876000	2.785344000
C	6.026531000	2.394314000	4.952473000
C	6.865450000	3.833468000	3.706632000
C	8.792143000	6.683847000	2.864586000
C	8.662682000	6.867662000	1.500201000
C	5.256022000	1.217434000	5.443514000
C	7.241643000	4.925471000	1.411543000
C	7.878533000	5.973947000	0.768512000
H	5.560157000	5.849024000	5.860730000
H	9.456433000	7.606107000	6.165095000
H	11.414206000	4.189934000	8.425448000
H	9.232396000	4.985453000	7.641435000
H	6.040798000	9.694206000	7.666443000
H	8.481865000	9.577642000	7.249857000
H	12.742650000	3.831403000	4.370325000
H	10.563949000	4.597102000	3.583563000
H	4.592226000	7.807673000	6.970026000
H	13.195249000	3.615603000	6.797884000
H	9.377000000	7.343505000	3.487461000
H	9.164430000	7.694909000	1.022813000
H	5.361630000	1.128096000	6.521708000
H	5.615053000	0.300271000	4.975845000
H	4.198565000	1.318244000	5.197728000
H	6.621388000	4.216506000	0.885174000
H	7.765078000	6.102527000	-0.298810000

The TD-DFT studies were performed in vacuo using Gaussian 09 c (DFT) CAM-B3LYP functional and 6-311++G(3d, 3p) basis set.[4, 5] The simulation of the first 8 excited states provided the following UV/vis absorption spectrum.

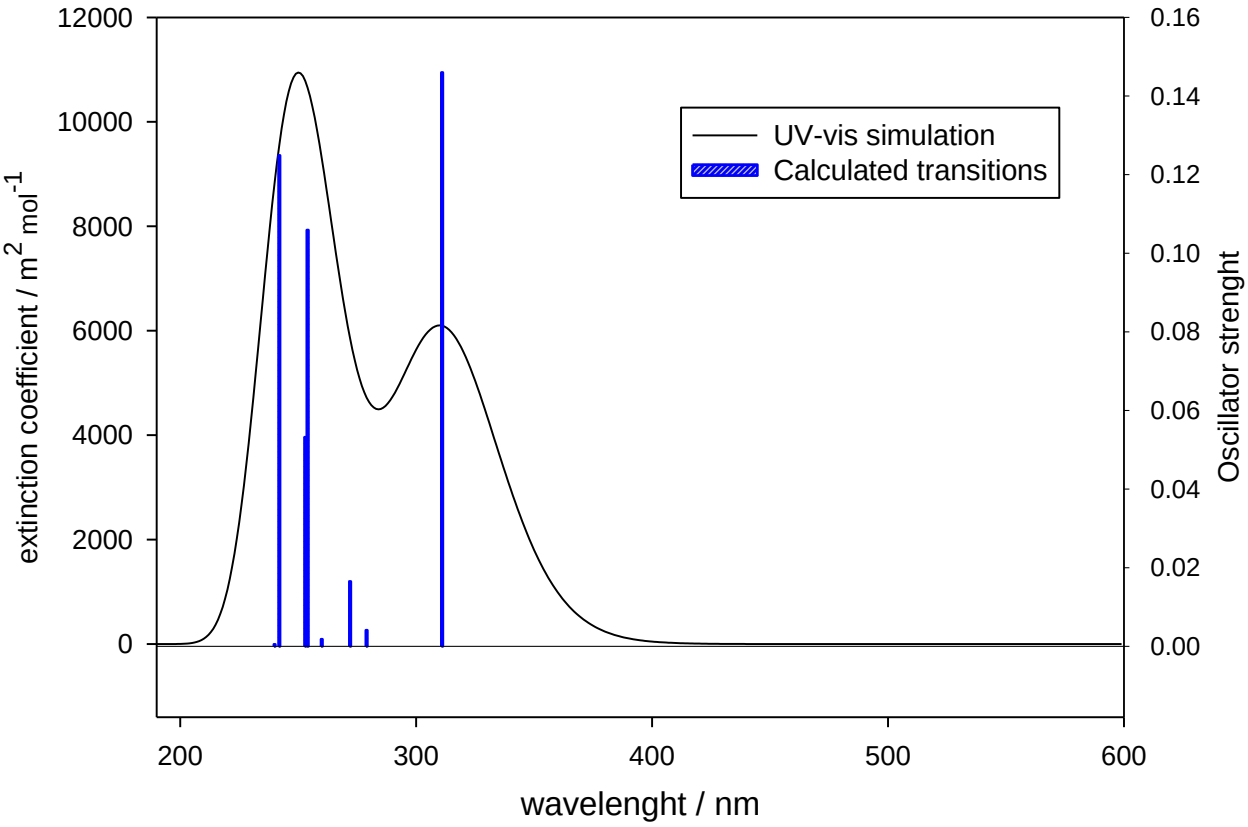

Figure 1: TDDFT calculated UV/vis absorption spectrum of the 1e (black line). The blue vertical lines correspond to the excitation transition calculated using TD-DFT/CAM-B3LYP/6-311++G(3d, 3p).

EES number (type)	Transition Energy nm (eV)	M.O. (contribution %)	Oscillator strength
1 (singlet)	311.62 (3.9787)	HOMO -3 -> LUMO (16 %) HOMO -1 -> LUMO (37 %) HOMO -> LUMO (38 %)	0.1460
2 (singlet)	279.55 (4.4351)	HOMO -3 -> LUMO (6 %) HOMO -2 -> LUMO (9 %) HOMO -1 -> LUMO (33 %) HOMO -> LUMO (46 %)	0.0041
3 (singlet)	272.03 (4.5577)	HOMO -4 -> LUMO (3 %) HOMO -3 -> LUMO (45 %) HOMO -2 -> LUMO (27 %) HOMO -1 -> LUMO (9 %) HOMO -> LUMO (7 %)	0.0165
4 (singlet)	260.36 (4.7621)	HOMO -3 -> LUMO (21 %) HOMO -2 -> LUMO (58 %) HOMO -1 -> LUMO (13 %) HOMO -> LUMO (3 %)	0.0018
5 (singlet)	254.88 (4.8645)	HOMO -4 -> LUMO (23 %) HOMO -3 -> LUMO (6 %) HOMO - 3 -> LUMO+1 (7 %) HOMO -1 -> LUMO+1 (26 %) HOMO -> LUMO+1 (28 %)	0.1059
6 (singlet)	253.48 (4.8914)	HOMO -4 -> LUMO (66 %) HOMO -3 -> LUMO+1 (4 %) HOMO -1 -> LUMO+1 (14 %) HOMO -> LUMO+1 (9 %)	0.0532
7 (singlet)	242.91 (5.1041)	HOMO -5 -> LUMO (89 %) HOMO -3 -> LUMO+1 (2 %)	0.1249
8 (singlet)	240.97 (5.1453)	HOMO -6 -> LUMO (66 %) HOMO -6 -> LUMO+1 (12 %) HOMO -6 -> LUMO+22 (3 %) HOMO -1 -> LUMO+1 (4 %) HOMO -> LUMO+1 (6 %)	0.0005

Table S2: Details of orbitals involved in excitation calculated by TD-DFT/CAM-B3LYP/6-311++G(3d, 3p). The transition energy is reported in wavelength and in electron volts. The contribution of each molecular orbital (M.O.) to the electronic transition is shown in the third column. The fourth column shows the oscillator strength.

First transition major MO:

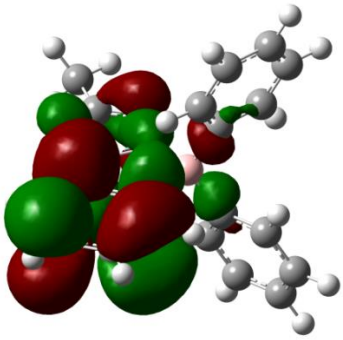

LUMO

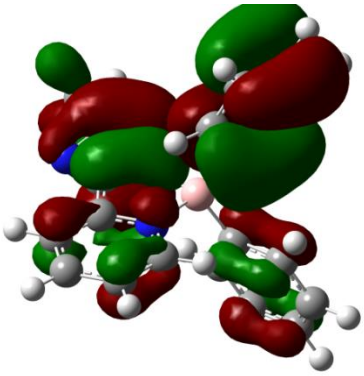

HOMO

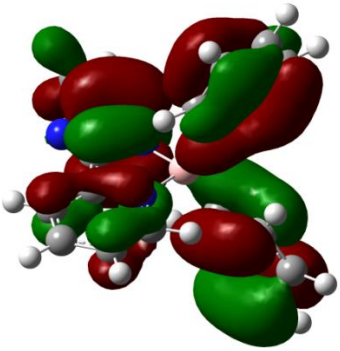

HOMO-1

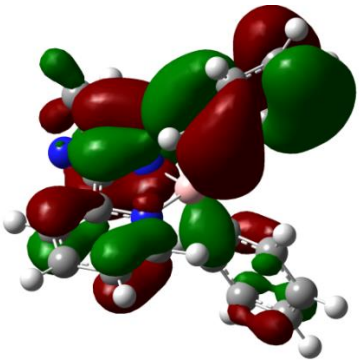

HOMO-3

Fig S27 Plots of the molecular orbitals involved in the longest wavelength excitation (311 nm) calculated with TD-DFT/CAM-B3LYP/6-311++G(3d, 3p).

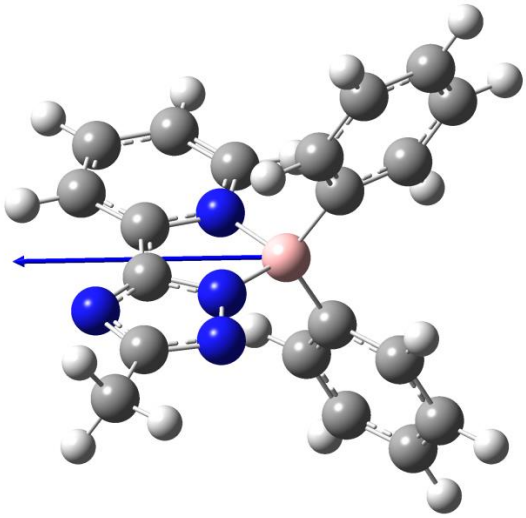

Fig. S28 Depiction of the **1e** and the dipole moment (blue arrow) in the first excited state (i.e. upon excitation at 311 nm) calculated by TD-DFT/rCAM-B3LYP/6-311++G(3d, 3p). EES1: 2.15 D.

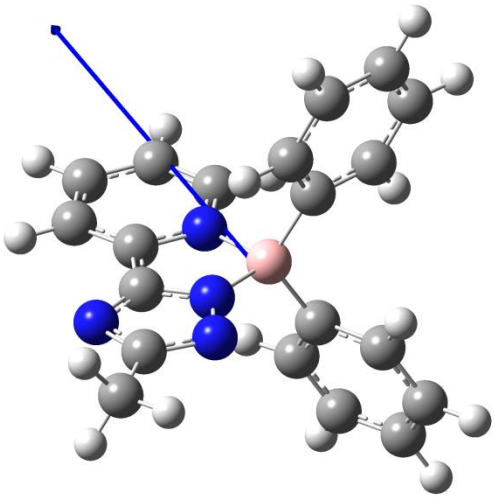

Fig. S29 Depiction of the **1e** and the dipole moment (blue arrow) in the ground state before excitation at 311 nm, calculated by DFT/rB3LYP/6-311++G(3d, 3p). GS: 5.75 D.

[1] Bruker. *APEX2 (v2012.4-3), SAINT (Version 8.18C) and SADABS (Version 2012/1). Bruker AXS Inc., Madison, Wisconsin, USA.* 2012

[2] G. Sheldrick, *Acta Crystallographica Section A,* 2008, **64**, 112

[3] Gaussian 09, Revision C, M. J. Frisch, G. W. Trucks, H. B. Schlegel, G. E. Scuseria, M. A. Robb, J. R. Cheeseman, G. Scalmani, V. Barone, B. Mennucci, G. A. Petersson, H. Nakatsuji, M. Caricato, X. Li, H. P. Hratchian, A. F. Izmaylov, J. Bloino, G. Zheng, J. L. Sonnenberg, M. Hada, M. Ehara, K. Toyota, R. Fukuda, J. Hasegawa, M. Ishida, T. Nakajima, Y. Honda, O. Kitao, H. Nakai, T. Vreven, J. A. Montgomery, Jr., J. E. Peralta, F. Ogliaro, M. Bearpark, J. J. Heyd, E. Brothers, K. N. Kudin, V. N. Staroverov, R. Kobayashi, J. Normand, K. Raghavachari, A. Rendell, J. C. Burant, S. S. Iyengar, J. Tomasi, M. Cossi, N. Rega, J. M. Millam, M. Klene, J. E. Knox, J. B. Cross, V. Bakken, C. Adamo, J. Jaramillo, R. Gomperts, R. E. Stratmann, O. Yazyev, A. J. Austin, R. Cammi, C. Pomelli, J. W. Ochterski, R. L. Martin, K. Morokuma, V. G. Zakrzewski, G. A. Voth, P. Salvador, J. J. Dannenberg, S. Dapprich, A. D. Daniels, Ö. Farkas, J. B. Foresman, J. V. Ortiz, J. Cioslowski, and D. J. Fox, Gaussian, Inc., Wallingford CT, 2009.
4 E. Runge and E. K. U. Gross, *Phys. Rev. Lett.*, 1984, **52**, 997.
5 T. Yanai, D. P. Tew and N. C. Handy, *Chem. Phys. Lett.* 2004, **393**, 51.